Acta Crystallographica Section F
Structural Biology Communications
ISSN 2053-230X

Expression, purification and preliminary crystallographic analysis of the cryptic polo-box domain of *Caenorhabditis elegans* ZYG-1

Ekaterina Shimanovskaya and Gang Dong*

Department of Medical Biochemistry, Max F. Perutz Laboratories, Medical University of Vienna, Dr Bohr-Gasse 9, 1030 Vienna, Austria

Correspondence e-mail: gang.dong@meduniwien.ac.at

Received 3 June 2014
Accepted 10 July 2014

ZYG-1 is a polo-like kinase essential for centriole assembly in *Caenorhabditis elegans*. The targeting of ZYG-1 to nascent centrioles is *via* its central cryptic polo-box (CPB) domain. To shed light on the molecular basis of ZYG-1 recruitment, it is necessary to obtain structural knowledge of the ZYG-1 CPB. Here, the expression, purification and preliminary crystallographic analysis of the ZYG-1 CPB are reported. The protein was overexpressed in *Escherichia coli* strain BL21 (DE3), purified by multi-step chromatography and crystallized using the vapour-diffusion method. Crystals of the wild-type protein exhibited an order–disorder pathology, which was solved by reductive lysine methylation. A complete anomalous data set was collected to 2.54 Å resolution at the Se *K* edge (λ = 0.9792 Å). The crystal belonged to space group *P*2, with unit-cell parameters $a = 53.3$, $b = 60.09$, $c = 87.51$ Å, $\beta = 93.31^\circ$. There were two molecules in the asymmetric unit.

1. Introduction

Centrioles are fascinating structures possessing an unusual ninefold symmetry. They are present in almost all eukaryotic cells and play essential roles both in forming centrosomes and in nucleating cilia and flagella. Research on centriole duplication in *Caenorhabditis elegans* over the past decade has led to the identification of a core set of centriolar proteins, of which one is the polo-like kinase ZYG-1 (UniProtKB/Swiss-Prot Q9GT24; O'Connell *et al.*, 2001).

ZYG-1 (and its orthologue Plk4) consists of three domains: a highly conserved N-terminal kinase domain, a central cryptic polo-box (CPB) domain and a C-terminal polo-box domain (Fig. 1*a*). It has been shown that both ZYG-1 and Plk4 target procentrioles *via* their CPB, which specifically interacts with an acidic region in SPD-2/Cep192 and/or asterless/Cep152 (Sonnen *et al.*, 2013; Hatch *et al.*, 2010; Cizmecioglu *et al.*, 2010; Dzhindzhev *et al.*, 2010). Recently, the crystal structure of the *Drososphila melanogaster* Plk4 CPB was solved and was shown to contain two tandem polo boxes, each consisting of six β-strands and one α-helix (Slevin *et al.*, 2012). Although believed to play similar roles during centriole assembly, the CPBs of Plk4 and ZYG-1 possess a very low sequence identity of only 17%. This prompted a debate as to whether ZYG-1 is a *bona fide* Plk4 orthologue or a structurally distinct counterpart in nematodes (Jana *et al.*, 2012; Slevin *et al.*, 2012; Cunha-Ferreira *et al.*, 2013). To obtain a direct structural comparison between ZYG-1 and the canonical Plk4, and to shed light on how the ZYG-1 CPB interacts with *C. elegans* SPD-2, it is necessary to determine a high-resolution structure of this domain.

In this study, we present a protocol for purification and crystallization of the ZYG-1 CPB and report the preliminary results of our X-ray diffraction experiments. Our work additionally demonstrates a potential application of reductive lysine methylation to overcome obstacles associated with pathological crystal packing of proteins.

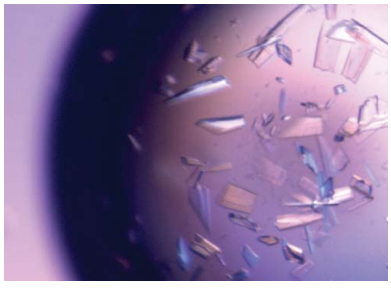

2. Materials and methods

2.1. Macromolecule production

Based on results from the protein secondary-structure-prediction software *POLYVIEW-2D* (Fig. 1*a*; Porollo *et al.*, 2004), various

protein constructs of the ZYG-1 CPB were designed. For cloning, positions of the forward and reverse PCR primers were chosen with respect to the predicted start or end of secondary-structure elements, either immediately before or 5–15 residues away. All cloned fragments were amplified by PCR using *C. elegans* cDNA as the template. The PCR products were digested using *Nco*I and *Bam*HI restriction enzymes and were subsequently ligated into a custom vector which provides an N-terminal 6×His tag cleavable by thrombin (leaving three amino acids, GSM, at the N-terminus of the target protein). The correct DNA sequence was confirmed by sequencing.

Various ZYG-1 CPB constructs were overexpressed in *Escherichia coli* BL21(DE3) cells. Cells were grown at 310 K until the OD_{600} reached 0.6–0.8 and were then incubated on ice for 15 min (cold shock) before shifting to 289 K for overnight expression of target proteins. Protein expression was induced with 0.5 m*M* isopropyl *β*-D-1-thiogalactopyranoside. Cells were harvested by centrifugation (5000*g*, 12 min) and resuspended in cold lysis buffer [20 m*M* Tris–HCl pH 8.0, 300 m*M* NaCl, 20 m*M* imidazole, 5%(*v*/*v*) glycerol, 15 m*M* *β*-mercaptoethanol]. Cell lysis was carried out using an EmulsiFlex-C3 homogenizer (Avestin Europe GmbH) and the lysate was cleared by centrifugation (15 000*g*, 40 min). The supernatant was filtered through a 0.45 µm nitrocellulose filter and loaded onto an Ni-HiTrap column (GE Healthcare Life Sciences) pre-equilibrated with the same lysis buffer. The column was washed with five column volumes (CV) of lysis buffer followed by 5 CV lysis buffer supplemented with 70 m*M* imidazole to remove bacterial contaminants (Guo *et al.*, 2007). Bound protein was eluted by a linear concentration gradient of imidazole (70–500 m*M*, 15 CV) in the same lysis buffer. The N-terminal 6×His tag was removed by incubation with 2%(*w*/*w*) thrombin overnight at 277 K. The sample was subsequently loaded onto a Superdex 200 16/60 size-exclusion column (GE Healthcare Life Sciences) pre-equilibrated with a buffer consisting of 20 m*M* Tris–HCl pH 8.0, 100 m*M* NaCl, 5%(*v*/*v*) glycerol, 1 m*M* dithiothreitol (DTT). Purification of the selected construct (residues 338–564) (Table 1) yielded a relatively higher amount of protein (2–4 mg per litre of of cell culture) than other constructs (less than 0.5 mg per litre of cell culture; data not shown).

For *de novo* phasing exploiting anomalous signals, selenomethionine (SeMet)-substituted ZYG-1 CPB (residues 338–564; Table 1) was expressed using M9 minimal medium supplemented with 19 amino acids (2 mg ml^{-1}) excluding methionine (Doublié, 1997). Prior to induction, 80 mg L-SeMet, 100 mg each of threonine, lysine and phenylalanine and 50 mg each of leucine, isoleucine and valine were added per litre of cell culture. The protein was purified as described above using the same buffer supplemented with 15 m*M* *β*-mercaptoethanol (for Ni-HiTrap chromatography) or 10 m*M* DTT (for size-exclusion chromatography).

Wild-type protein gave rise to rod-shaped crystals, but the crystals had an order–disorder pathology in molecular packing (see §3). Attempts to alter the crystal packing using various truncations of the protein were unsuccessful (data not shown). As such, an additional step of reductive lysine methylation (Sledz *et al.*, 2010) was implemented in the hope of identifying an improved crystal packing by modifying the intermolecular contacts in the crystal. In this protocol, after purification by affinity chromatography on Ni-HiTrap the sample was run on a HiPrep 26/10 desalting column (GE Healthcare Life Sciences) equilibrated with 50 m*M* HEPES–NaOH pH 7.5, 250 m*M* NaCl to accomplish buffer exchange. The protein was diluted to a final concentration of ∼1 mg ml^{-1}. To methylate lysine residues of the protein, 20 µl freshly prepared 1 *M* dimethylamine–borane complex (ABC; Sigma–Aldrich) and 40 µl 1 *M* formaldehyde (Fluka–Sigma–Aldrich) were added per millilitre of protein solution. The reaction was incubated at 277 K for 2 h with continuous gentle stirring. Subsequently, a further 20 µl ABC and 40 µl formaldehyde were added to each millilitre of protein solution and the reaction mixture was stirred for a further 2 h. Following a final addition of 10 µl ABC per millitre of protein solution, the reaction was stirred overnight at 277 K. Upon completion of the reaction, the protein was concentrated and loaded onto a Superdex 200 16/60 column (GE Healthcare Life Sciences) pre-equilibrated with 20 m*M* Tris–HCl pH 8.0, 100 m*M* NaCl, 5%(*v*/*v*) glycerol, 10 m*M* DTT (Fig. 1*b*). Fractions containing the target protein were pooled and the protein was concentrated by

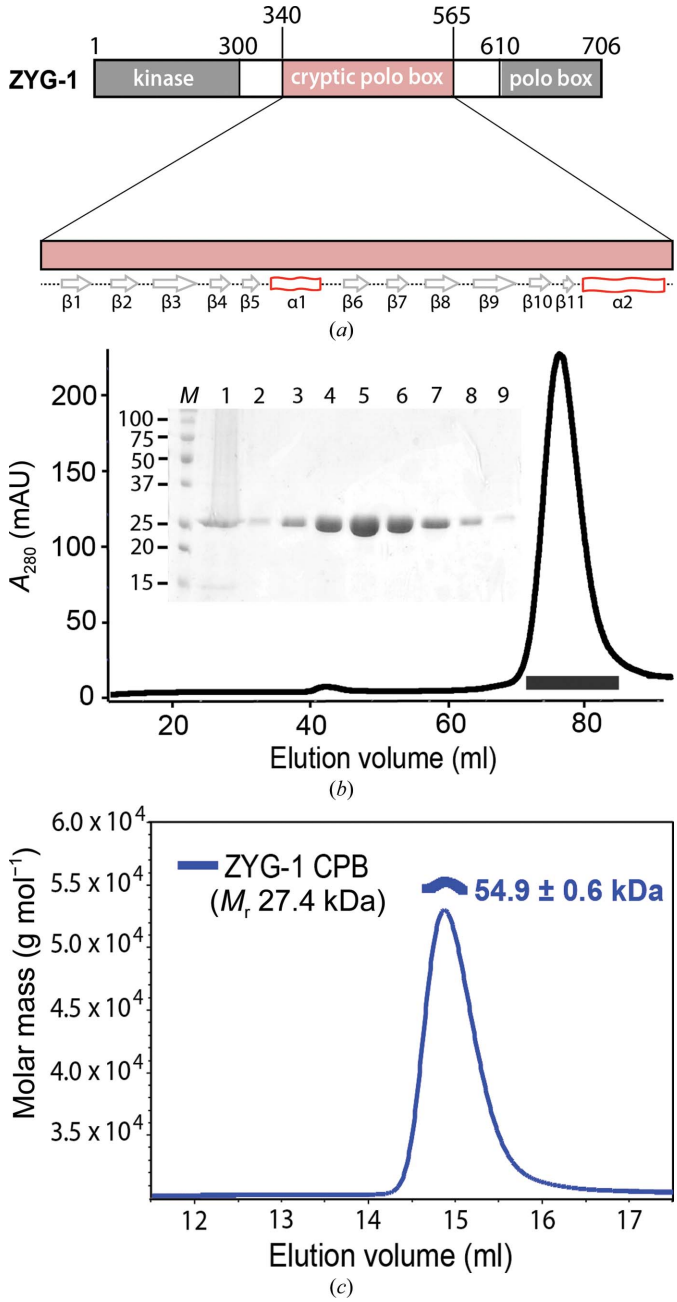

Figure 1
Cloning and purification of the ZYG-1 CPB. (*a*) Domain organization of ZYG-1 and secondary-structure predictions of the ZYG-1 CPB. (*b*) Elution profile of the lysine-methylated SeMet-ZYG-1-CPB (residues 338–564) from a Superdex S200 16/60 size-exclusion column. Fractions of the elution peak were checked using SDS–PAGE. Lane *M*, molecular-mass marker; lane 1, 1% of the input sample; lanes 2–9, elution fractions at the peak (horizontal bar). (*c*) Static light-scattering results showing that the ZYG-1 CPB forms a dimer in solution.

Table 1
Cloning of *C. elegans* ZYG-1 CPB.

Restriction sites in the primers are underlined. The 6×His tag and the thrombin cleavage site in the amino-acid sequence are shown in italic and underlined, respectively.

Source organism	*C. elegans*
DNA source	cDNA
Forward primer	5′-GCTGCCATGGGTDCCGTACCTCCAAGC-3′
Reverse primer	5′-CGACGGATCCTCAAGCCAACCATATTAGTTCCTG-3′
Cloning and expression vector	HM-15b (derived from pET-15b; Novagen)
Expression host	*E. coli*
Complete amino-acid sequence of the construct produced	MSS*HHHHHH*SSGLVPRGSMGTVPPSREDRNSQLWPIRMDRLE-GSMGTVPPSREDRNSQLWPIRMDRLEGQRVCTAGGRYIVE-LDTRCRFEVAAQGNFVKRILIVEVDEMVQTVYVHRIPDRT-VRGRNGEEELITLTNNPFVYTSYSQMPKEVQNDYMRLQKM-VAVTISGRVAKVTFRRPSQFPDAQAQLMENGDLRIKLPRS-VIVRKMDNGEIFNCIDGIATQKQAVSGITLTKVNEVYKYL-IRFEQCLNGMDRGMVCFPIVFSAGTNMV

centrifugation in an Ultra-15 Centrifugal Filter Unit with a 10 kDa molecular-weight cutoff (EMD Millipore Amicon). The protein sample, which was at approximately 10 mg ml^{-1} as estimated by SDS–PAGE, was used directly for crystallization trials. Excess samples were divided into aliquots and stored at 193 K until further use. All chromatographic runs were carried out at 277 K.

Static light scattering was used to determine the oligomerization state of the ZYG-1 CPB. The experiments were carried out on a miniDAWN TREOS light-scattering instrument coupled to a 1260 Infinity HPLC system (Agilent Technologies) and a Superdex 200 10/300 GL gel-filtration column (GE Healthcare Life Sciences). Prior to sample loading, the system was pre-equilibrated overnight at room temperature with a buffer consisting of 20 m*M* Tris–HCl pH 8.0, 100 m*M* NaCl, 10 m*M* DTT. 80 µl SeMet-substituted ZYG-1 CPB (1 mg ml^{-1}) was loaded onto the column. The Wyatt *Astra* software (v.5.3.4.14) was used for data analysis. The weight-averaged molar mass of the elution peak was calculated using the collected light-scattering and refractive-index data.

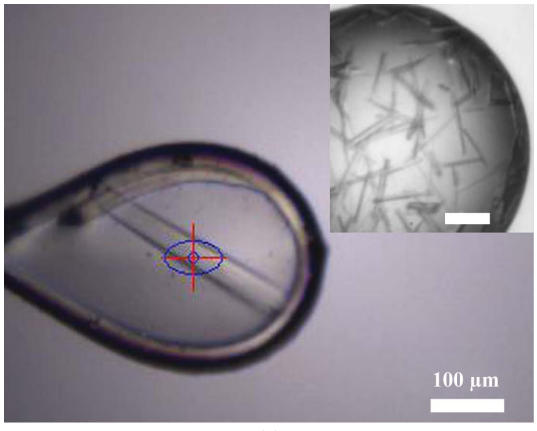

(*a*)

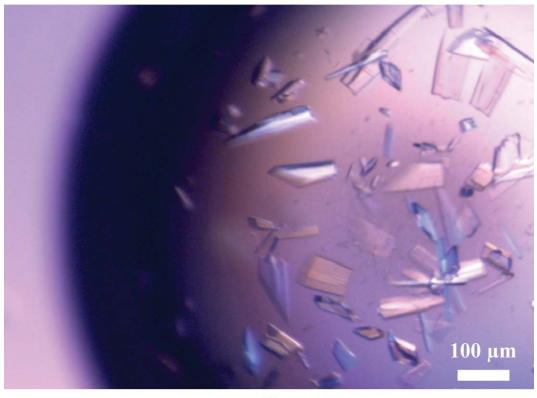

(*b*)

Figure 2
Crystals of wild-type and lysine-methylated SeMet-ZYG-1 CPB. (*a*) Picture of the rod-like crystals of wild-type ZYG-1 CPB (residues 338–564). (*b*) Picture of the plate-like crystals of lysine-methylated SeMet-ZYG-1 CPB (residues 338–564)

Table 2
Crystallization information.

Protein	Wild-type ZYG-1 CPB	Lysine-methylated SeMet-ZYG-1 CPB
Method	Hanging drop	Hanging drop
Plate type	48-well plate (Hampton Research)	48-well plate (Hampton Research)
Temperature (K)	295	295
Protein concentration (mg ml^{-1})	5	10
Buffer composition of protein solution	20 m*M* Tris–HCl pH 8.0, 100 m*M* NaCl, 5%(*v*/*v*) glycerol, 5 m*M* DTT	20 m*M* Tris–HCl pH 8.0, 100 m*M* NaCl, 5%(*v*/*v*) glycerol, 5 m*M* DTT
Composition of reservoir solution	0.1 *M* HEPES–NaOH pH 7.5, 0.2 *M* $CaCl_2$, 28%(*v*/*v*) PEG 4000	0.1 *M* trisodium citrate pH 5.6, 15%(*w*/*v*) PEG 4000, 0.2 *M* ammonium sulfate
Volume and ratio of drop	3 µl (2:1)	3 µl (2:1)
Volume of reservoir (µl)	200	200

2.2. Crystallization

The screening of crystallization conditions was performed at both 277 and 295 K using three commercial crystallization kits: Crystal Screen HT (Hampton Research), Cryo 1&2 (Emerald Bio) and JBScreen Classic 1–4 (Jena Bioscience). All conditions were dispensed by a Crystal Phoenix Robot (Art Robbins Instruments) into two-well MRC plates (Hampton Research) using protein:mother liquor ratios of 100:100 nl and 200:100 nl. Rod-like crystals of wild-type CPB appeared in numerous conditions from JBScreen 1–4 after overnight incubation at both 277 and 295 K. These conditions typically contained polyethylene glycol (PEG). Rod-like crystals grown in a reservoir solution consisting of 0.1 *M* HEPES–NaOH pH 7.5, 0.2 *M* $CaCl_2$, 28%(*v*/*v*) PEG 400 reached maximum dimensions of 50 × 50 × 500 µm after 3 d (Fig. 2*a*). All conditions yielding large crystals contained variable amounts of PEG 4000 or PEG 8000 as the precipitant and $MgCl_2$ or $CaCl_2$ as the additive in the pH range 7.5–9.5 in either Tris–HCl or HEPES–NaOH buffer (Table 2). The rod-like crystals diffracted X-rays to maximally 2.8 Å resolution and had characteristic diffuse streaks in alternating layers (Fig. 3*a*). The Hampton Research Additive Screen was used to search for an altered crystal packing. Unfortunately, none of the additives led to an improved diffraction pattern (data not shown). To determine the influence of cooling procedures on crystal quality, in-house X-ray diffraction experiments in capillaries at room temperature were performed (Balaic *et al.*, 1996). No significant change in the diffraction images was observed (data not shown).

Implementation of the reductive lysine-methylation step resulted in thin plate-like crystals. The crystals grew at 295 K in conditions consisting of either 0.1 *M* Tris–HCl pH 8.5, 16%(*w*/*v*) PEG 4000, 0.2 *M* Li_2SO_4 or 0.1 *M* sodium citrate pH 5.6, 15%(*w*/*v*) PEG 4000, 0.2 *M* ammonium sulfate. Finally, lysine-methylated SeMet-substituted *C. elegans* ZYG-1 CPB (residues 338–564) was crystallized at 295 K by the hanging-drop technique against reservoir solution consisting of 0.1 *M* trisodium citrate pH 5.6, 15%(*w*/*v*) PEG 4000, 0.2 *M* ammonium sulfate. Each crystallization droplet contained 2 µl protein sample and 1 µl reservoir solution (Table 2). Small plate-like crystals appeared after 2 d and reached maximal

dimensions of 10 × 100 × 100 µm after 5 d (Fig. 2*b*). Prior to cooling in liquid nitrogen, the crystals were soaked in the same reservoir solution containing increasing amounts of glycerol to a final concentration of 20%(*v*/*v*).

2.3. Data collection and processing

A diffraction data set was collected to ∼2.5 Å resolution on beamline ID14-4 at the European Synchrotron Radiation Facility (ESRF), Grenoble, France (Fig. 3*b*). The data set was collected at the *K* edge of selenium (λ = 0.9792 Å; Table 3) and was processed using the *XDS* data-processing suite (Kabsch, 2010) followed by *POINTLESS* and *SCALA* (Evans, 2006).

3. Results and discussion

The *C. elegans* ZYG-1 CPB (residues 338–564) was successfully overexpressed and purified from the *E. coli* BL21(DE3) expression system. Soluble protein constructs were purified using a two-step purification protocol comprising affinity purification followed by size-exclusion chromatography. Initial attempts at protein purification produced a sample contaminated with the bacterial chaperone protein DnaK (70 kDa). To eliminate the DnaK contamination, additional washes with the lysis buffer containing 70 m*M* imidazole during the affinity-purification step were used (Guo *et al.*, 2007), which allowed us to obtain >95% pure protein sample as judged by SDS–PAGE (Fig. 1*b*). Similar to the Plk4 CPB (Slevin *et al.*, 2012), the ZYG-1 CPB formed a dimer in solution as confirmed by static light scattering (Fig. 1*c*).

Purified proteins were easily crystallized in multiple conditions (Fig. 2*a*). Unfortunately, the protein structure could not be solved owing to the poor quality of the X-ray diffraction data caused by

Table 3
Data-collection and processing statistics.

Values in parentheses are for the outer shell.

Diffraction source	ID14-4, ESRF
Wavelength (Å)	0.9792
Temperature (K)	100
Detector	ADSC Q315r CCD
Crystal-to-detector distance (mm)	334.14
Rotation range per image (°)	0.95
Total rotation range (°)	190
Exposure time per image (s)	1.7
Space group	*P*121
a, *b*, *c* (Å)	53.38, 60.09, 87.51
α, β, γ (°)	90, 93.31, 90
Mosaicity (°)	0.65
Resolution range (Å)	50.0–2.54 (2.69–2.54)
Total No. of reflections	18224 (2793)
No. of unique reflections	4746 (709)
Completeness (%)	97.4 (96.3)
Multiplicity	3.84 (3.94)
$\langle I/\sigma(I)\rangle$	10.87 (2.82)
$R_{\rm r.i.m.}$ (%)	10.0 (69.7)
Overall *B* factor from Wilson plot (Å^2)	25.52
No. of molecules per asymmetric unit	2
$V_{\rm M}$ (Å^3 Da^{-1})	2.56
Solvent content (%)	52.0

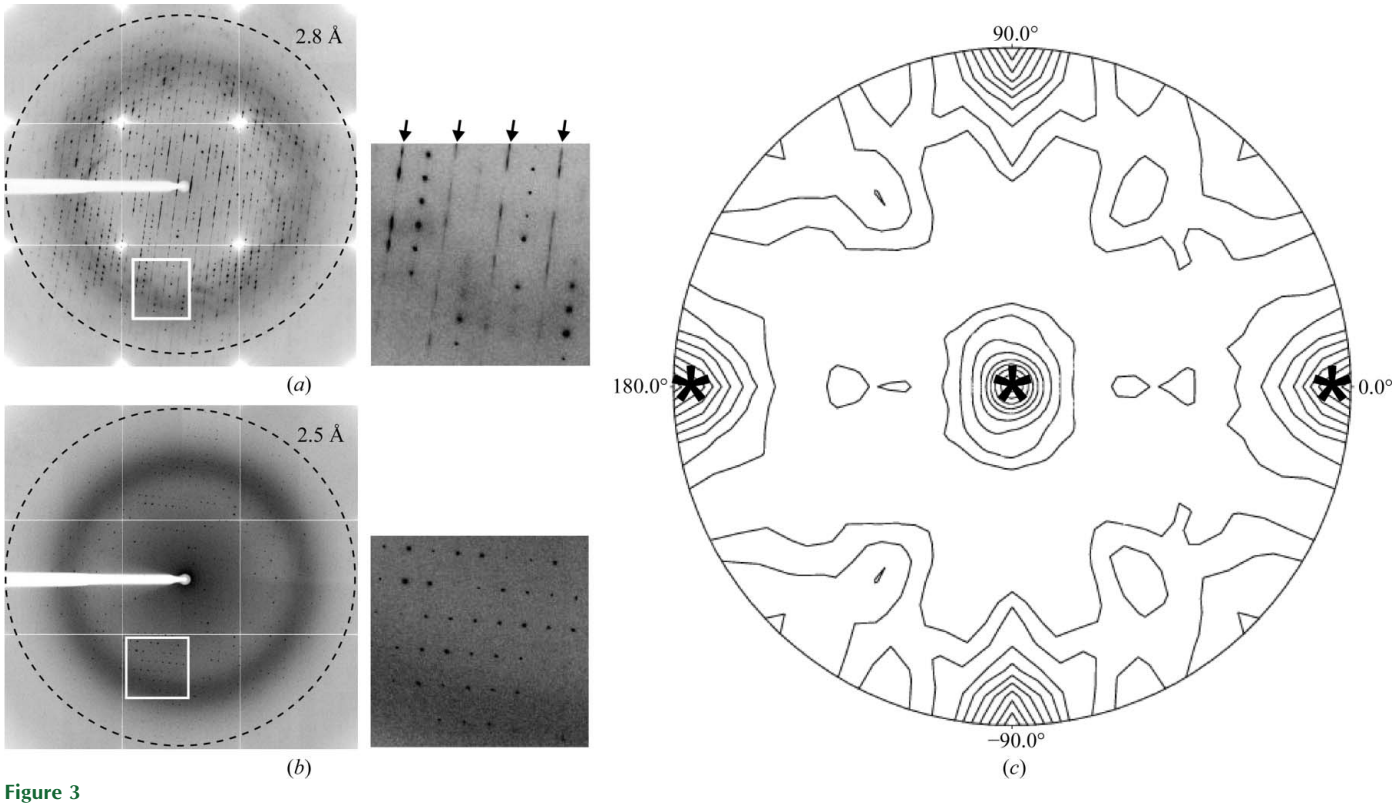

Figure 3
X-ray diffraction images recorded for wild-type ZYG-1 CPB and lysine-methylated SeMet-ZYG-1 CPB. (*a*) X-ray diffraction image of a rod-like crystal of the wild-type ZYG-1 CPB as shown in Fig. 2(*a*). The right panel shows an enlarged view of the boxed region in the diffraction image on the left. The characteristic diffuse streaks in alternating layers of the diffraction are marked by arrows. (*b*) X-ray diffraction image of a crystal of lysine-methylated SeMet-ZYG-1 CPB as shown in Fig. 2(*b*). The right panel shows an enlarged view of the boxed region in the diffraction image. (*c*) Stereographic projection of the self-rotation function calculated from diffraction data of lysine-methylated SeMet-ZYG-1 CPB at κ = 180°. The horizontal and vertical polar coordinates of the rotation axis are ω (0–90° from the centre to the edge of the circle) and φ (plotted around the circumference). The peaks at the top and the bottom of the plot are from the crystallographic twofold axis. The other peaks (marked by asterisks) represent twofold noncrystallographic symmetry axes.

lattice-translational defects in the crystal lattice (Fig. 3*a*). This type of defect occurs owing to a consistent shift between successive layers of macromolecules arising during crystal formation (Pletnev *et al.*, 2009). All attempts to alter the crystal packing by using multiple protein truncations and numerous additives in crystallization were unsuccessful.

Reductive lysine methylation is a commonly used approach for facilitating and enhancing the crystallization of biological macromolecules (Kim *et al.*, 2008). Since the ZYG-1 CPB construct contained nine lysine residues (Table 1), it was decided to implement a lysine-methylation step prior to crystallization trials. After lysine methylation, crystals of a different morphology were obtained in a crystallization condition consisting of 0.1 *M* trisodium citrate pH 5.6, 15%(*w*/*v*) PEG 4000, 0.2 *M* ammonium sulfate (Table 2). The plate-like crystals (Fig. 2*b*) diffracted X-rays to maximally 2.5 Å resolution and without pathological diffuse streaks in the diffraction pattern (Fig. 3*b*). A complete data set was collected at the Se *K* edge (Table 3). Assuming that there are two monomers in the asymmetric unit, the Matthews coefficient (V_M; Matthews, 1968) was calculated to be 2.56 $Å^3$ Da^{-1} and the estimated solvent content was 52.0% (Table 2). The self-rotation function was calculated between 10 and 4 Å resolution with an integration radius of 20 Å. Peaks representing twofold noncrystallographic symmetry axes are visible in the $\kappa = 180^\circ$ section (Fig. 3*c*). The calculation was carried out with *POLARRFN* using the UCLA MBI Self Rotation Function Server (http://services.mbi.ucla.edu/selfrot/).

At present, structure determination of the ZYG-1 CPB is ongoing using single-wavelength anomalous dispersion methods. The solved structure of the ZYG-1 CPB will be compared with the reported *D. melanogaster* Plk4 CPB structure to elucidate the changes undergone by CPBs during evolution. The structure should also provide hints as to how it physically interacts with the acidic region of *C. elegans* SPD-2 during centriole assembly.

This research was supported by institutional support from the Max F. Perutz Laboratories and grant P23440-B20 from the Austrian Science Fund (FWF) to GD. We thank Dr Sandor Brockhauser for assistance with our data collection at the ESRF, Alexander Dammermann and Carrie Cowan for providing *C. elegans* cDNA and Brooke Morriswood for critical reading of the manuscript.

References

Balaic, D. X., Barnea, Z., Nugent, K. A., Garrett, R. F., Varghese, J. N. & Wilkins, S. W. (1996). *J. Synchrotron Rad.* **3**, 289–295.
Cizmecioglu, O., Arnold, M., Bahtz, R., Settele, F., Ehret, L., Haselmann-Weiss, U., Antony, C. & Hoffmann, I. (2010). *J. Cell Biol.* **191**, 731–739.
Cunha-Ferreira, I., Bento, I., Pimenta-Marques, A., Jana, S. C., Lince-Faria, M., Duarte, P., Borrego-Pinto, J., Gilberto, S., Amado, T., Brito, D., Rodrigues-Martins, A., Debski, J., Dzhindzhev, N. & Bettencourt-Dias, M. (2013). *Curr. Biol.* **23**, 2245–2254.
Doublié, S. (1997). *Methods Enzymol.* **276**, 523–530.
Dzhindzhev, N. S., Yu, Q. D., Weiskopf, K., Tzolovsky, G., Cunha-Ferreira, I., Riparbelli, M., Rodrigues-Martins, A., Bettencourt-Dias, M., Callaini, G. & Glover, D. M. (2010). *Nature (London)*, **467**, 714–718.
Evans, P. (2006). *Acta Cryst.* D**62**, 72–82.
Guo, L.-W., Assadi-Porter, F. M., Grant, J. E., Wu, H., Markley, J. L. & Ruoho, A. E. (2007). *Protein Expr. Purif.* **51**, 187–197.
Hatch, E. M., Kulukian, A., Holland, A. J., Cleveland, D. W. & Stearns, T. (2010). *J. Cell Biol.* **191**, 721–729.
Jana, S. C., Bazan, J. F. & Bettencourt Dias, M. (2012). *Structure*, **20**, 1801–1804.
Kabsch, W. (2010). *Acta Cryst.* D**66**, 125–132.
Kim, Y. *et al.* (2008). *Nature Methods*, **5**, 853–854.
Matthews, B. W. (1968). *J. Mol. Biol.* **33**, 491–497.
O'Connell, K. F., Caron, C., Kopish, K. R., Hurd, D. D., Kemphues, K. J., Li, Y. & White, J. G. (2001). *Cell*, **105**, 547–558.
Pletnev, S., Morozova, K. S., Verkhusha, V. V. & Dauter, Z. (2009). *Acta Cryst.* D**65**, 906–912.
Porollo, A. A., Adamczak, R. & Meller, J. (2004). *Bioinformatics*, **20**, 2460–2462.
Sledz, P., Zheng, H., Murzyn, K., Chruszcz, M., Zimmerman, M. D., Chordia, M. D., Joachimiak, A. & Minor, W. (2010). *Protein Sci.* **19**, 1395–1404.
Slevin, L. K., Nye, J., Pinkerton, D. C., Buster, D. W., Rogers, G. C. & Slep, K. C. (2012). *Structure*, **20**, 1905–1917.
Sonnen, K. F., Gabryjonczyk, A. M., Anselm, E., Stierhof, Y. D. & Nigg, E. A. (2013). *J. Cell Sci.* **126**, 3223–3233.